ASTRONOMY & ASTROPHYSICS
SUPPLEMENT SERIES

Astron. Astrophys. Suppl. Ser. **135**, 133–144 (1999)

First DENIS *I*-band extragalactic catalog⋆,⋆⋆

I. Vauglin[1], G. Paturel[1], J. Borsenberger[2], P. Fouqué[3,4], N. Epchtein[3,5], S. Kimeswenger[6], D. Tiphène[3], P. Lanoix[1], and H. Courtois[1]

[1] CRAL-Observatoire de Lyon, F-69561 Saint-Genis Laval Cedex, France
[2] Institut d'Astrophysique de Paris, 98 bis boulevard Arago, F-75014 Paris, France
[3] Observatoire de Paris-Meudon, F-92195 Meudon Principal Cedex, France
[4] European Southern Observatory, La Silla, La Serena, Chile
[5] Observatoire de Nice, Departement Fresnel, BP. 4429, F-06304 Nice Cedex, France
[6] Institut fur Astronomie, Technikerstrasse 25, A-6020 Innsbruck, Austria

Received August 7; accepted October 9, 1998

Abstract. This paper presents the first *I*-band photometric catalog of the brightest galaxies extracted from the Deep Near Infrared Survey of the Southern Sky (DENIS) An automatic galaxy recognition program has been developed to build this provisional catalog. The method is based on a discriminating analysis. The most discriminant parameter to separate galaxies from stars is proved to be the peak intensity of an object divided by its array. Its efficiency is better than 99%. The nominal accuracy for galaxy coordinates calculated with the Guide Star Catalog is about 6 arcsec. The cross-identification with galaxies available in the Lyon-Meudon Extragalactic DAtabase (LEDA) allows a calibraton of the *I*-band photometry with the sample of Mathewson et Al. Thus, the catalog contains total *I*-band magnitude, isophotal diameter, axis ratio, position angle and a rough estimate of the morphological type code for 20260 galaxies. The internal completeness of this catalog reaches magnitude $I_{\rm lim} = 14.5$, with a photometric accuracy of ~ 0.18 m. 25% of the Southern sky has been processed in this study.

This quick look analysis allows us to start a radio and spectrographic follow-up long before the end of the survey.

Key words: galaxies: general — catalogs — galaxies: photometry — surveys

Send offprint requests to: G. Paturel

⋆ Based on observations collected at the European Southern Observatory, La Silla, Chile.

⋆⋆ The catalogue is available at the CDS via anonymous ftp 130.79.128.5 or http://cdsweb.u-strasbg.fr/Abstract.html

1. Introduction

In Paturel et al. (1996), we presented our program of collecting the main astrophysical parameters for the principal galaxies. The first target was limited to adding information on galaxies already known in the LEDA database.

The work is now more ambitious because we are aiming at detecting new galaxies from the *Deep Near Infrared Survey of the Southern Sky* (hereafter DENIS). DENIS is a program to survey the entire southern sky in three wavelength bands (Gunn-*i*: 0.80 μm, *J*: 1.25 μm and Ks: 2.15 μm) with limiting magnitudes of 18.5, 16.5 and 14.0 respectively. The observations are performed with the ESO 1 m-telescope at La Silla (Chile) with a dedicated camera. The survey observations with three channels started in routine mode in December 1995. A detailed description of DENIS is given in Epchtein (1998) and in Garzón et al. (1997).

The systematic detection, extraction and cataloging of DENIS extragalactic sources are of significant interest for studies requiring large and homogeneous samples such as the kinematics of the local universe, the distance scale, cosmology etc. The *I*-band is the most suitable both for the detection of extended objects and for the star/galaxy separation, except in the galactic plane. Thus, in the present study only the *I*-band images are considered.

The transfer of DENIS images from Paris to Lyon is explained in Sect. 2 and the extraction of objects from these images in Sect. 3. In Sects. 4 to 5 we describe astrometry and automatic galaxy recognition and analysis. Then, in Sects. 6 to 8, we explain how galaxies are cross-identified with LEDA galaxies leading to the comparison of astrophysical parameters with those from Mathewson et al. and from LEDA. Finally, in Sect. 9 we describe the provisional *I*-band DENIS catalog.

It is important to note that a deeper catalog will be made at the end of the survey. Hence, the present catalog is a preliminary catalog of bright galaxies detected by DENIS, and used to start a radio and spectrographic follow-up long before the end of the survey. The present measurements cover one year of observation.

2. Obtaining I-band CCD frames from DENIS

2.1. Characteristics of the DENIS survey

The I-band of the survey is the Gunn-i band at 0.80 μm. The CCD camera is a Tektronix 1024×1024 pixel array cooled down to liquid nitrogen temperature. Each frame (768 × 768 pixels) represents 12 square arcminutes with a pixel size of 1 arcsec. The integration time is 9 s. The read-out noise is about 7 e^-. The observing strategy consists in scanning at a constant right ascension on strips of 30 degrees in declination (180 frames per strip) taken in three zones "Equatorial" from $\delta = +2$ deg to -28 deg, "Intermediate" from $\delta = -28$ deg to -58 deg and "Polar" from $\delta = -58$ deg to -88 deg. The overlap between adjacent frames is 1 arcmin on each side (i.e. 2 arcmin in each direction). This strategy aims at covering a wide range of airmasses. Each strip starts and ends with photometric and astrometric calibrations. At the end of some nights a flat fielding is performed directly on the sky during sunrise. The data is archived on DAT cartridges which are send each week to the *Paris Data Analysis Center* (PDAC) at the Institut d'Astrophysique de Paris for processing.

2.2. Pipeline Lyon-PDAC

A systematic automatic processing of DENIS I-images began in Lyon in February 1996. Flat-fielding and de-biasing are made at PDAC on each genuine frame. For the Lyons processing each I-image is reduced by a factor 4 in size by rebinning pixels 2 × 2. Our effective pixel size is thus 2 arcseconds. An example of an I-frame is given in Fig. 1.

The histogram of pixel intensities is used to calculate the sky background intensity $f_{\rm bg}$. The sky-background level is taken at the maximum intensity of the histogram (i.e. the mode) and the standard deviation σ is calculated by symmetrizing the low intensity part of the histogram with respect to the mode. The sources are concentrated in the high intensity part of the histogram.

A threshold is then applied (the threshold level is $f_{\rm bg} + 2.0\sigma$). Using this procedure (averaging and thresholding) allows a compression factor of 20 to 30, depending on the image contents. All images of a given I-strip are thus compressed, tar'd and automatically transferred to Lyon via ftp. A full strip is stored in 10 to 13 Mbytes. The galaxy extraction is made at Lyon using the program described in the following section.

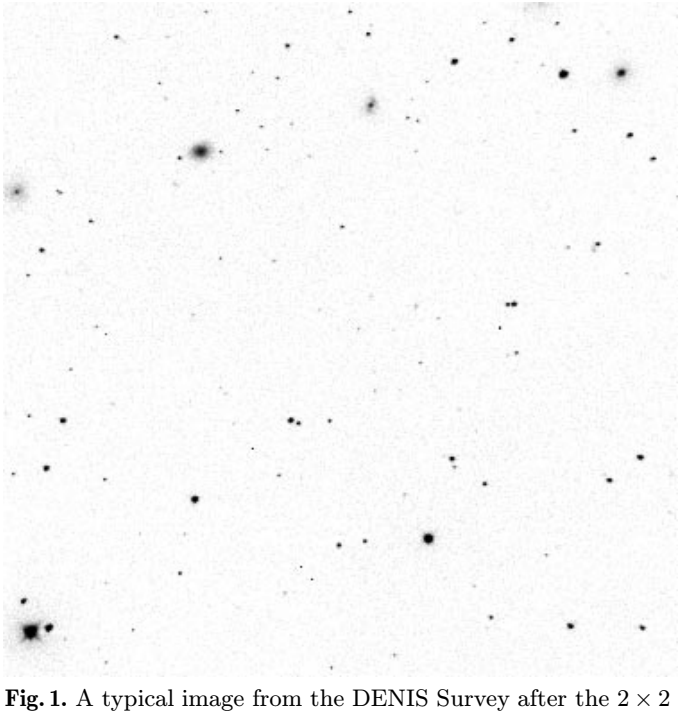

Fig. 1. A typical image from the DENIS Survey after the 2 × 2 rebinning. The frame is $12' \times 12'$. North is on the bottom side, East is on the left side. Among the four galaxies clearly visible on the top, one (the third from the left) is a new one. This shows that relatively bright galaxies can be discovered

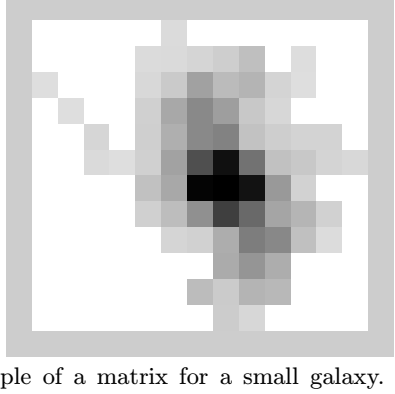

Fig. 2. Example of a matrix for a small galaxy. One pixel is $2'' \times 2''$. The edge is outside the matrix

3. Extraction of astronomical objects

All sources (stars, galaxies, defects etc.) are extracted using the same algorithm as described in Paturel et al. (1996, Sect. 3.1), except that no attempt was made to share interacting objects which are simply flagged after visual inspection (Sect. 5). The reason is that we are interested first of all in well defined objects. At the end of this stage, we obtain for each frame a collection of matrixes (see an example in Fig. 2). Matrixes smaller than 17 pixels are rejected. They correspond, to the mean, of objects of 6 arcsec in diameter.

Astrophysical parameters are extracted for each matrix according to Paturel et al. (1996, Sect. 3.2). These parameters are the following:

- Weighted mean position of the center $x_{\rm m}$ and $y_{\rm m}$ (in pixels), where the weight is the pixel intensity f_{ij}
- major axis $\log D$ (D in 0.1 arcmin) at faint isophotal level (external diameter).
- axis ratio $\log R$ (log of major to minor axis)
- position angle of the major axis β (in degrees, counted from North towards East)
- magnitude $I = -2.5 \log(\sum_{i=1}^{n} f_{ij} - f_{\rm bg}) + {\rm cst}$ (in arbitrary units), n is the number of pixels with intensity f_{ij} larger than the threshold.

We have now to perform astrometry (conversion of pixels positions to right ascension and declination) and then recognition of "galaxies", "stars", and "unknown objects".

4. Astrometry

The center of the frame is taken from the header of the FITS file. From the Guide Star Catalog (GSC) and from the LEDA database we extract all objects (stars or galaxies) known in the corresponding square. A cross-identification between matrixes and stars is made exactly as described in Paturel et al. (1996, Sects. 3.3 and 3.4). Galaxies are also used but only when they have accurate coordinates (i.e. typically better than 10 arcsec). A 6th order polynomial fit converts (x, y) positions on the frames to Right Ascension and Declination. The number of GSC stars varies from one frame to another. A histogram of number of GSC stars per frame is given in Fig. 3. If this number is smaller than 7 or if the standard deviation of the polynomial fit is greater than 4 arcsec, the solution is rejected and we adopt the "header" solution calculated from the coordinates of the center and the pixel size as given in the header. If the GSC-solution seems acceptable but differs from the header-solution by more than 30 arcsec, the header solution is preferred and coordinates are flagged to recall that they may be inaccurate.

In Fig. 4, we show the differences between the GSC-solution and the FITS header-solution. Most of them are in good agreement within 15 arcsec. Note that more recent measurements have been astrometrically calibrated to better than 1 arcsec by cross-identifying with the PMM database.

Galaxy coordinates will be compared directly with coordinates of LEDA galaxies.

5. Automatic star/galaxy separation

5.1. Test sample

A sample of 1146 objects has been visually classified into three classes: stars, galaxies and unknown objects. The distribution in each class is the following:

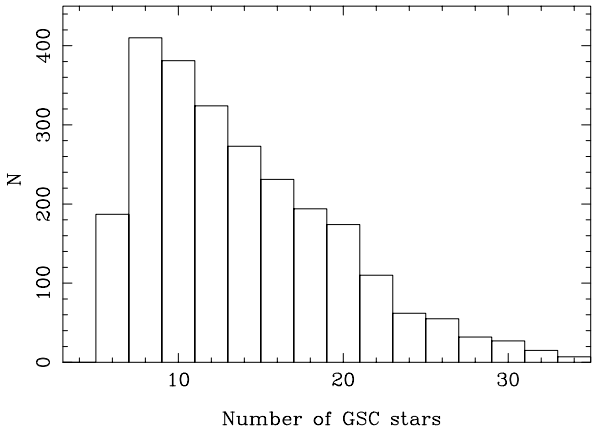

Fig. 3. Histogram of the number of GSC stars by frame

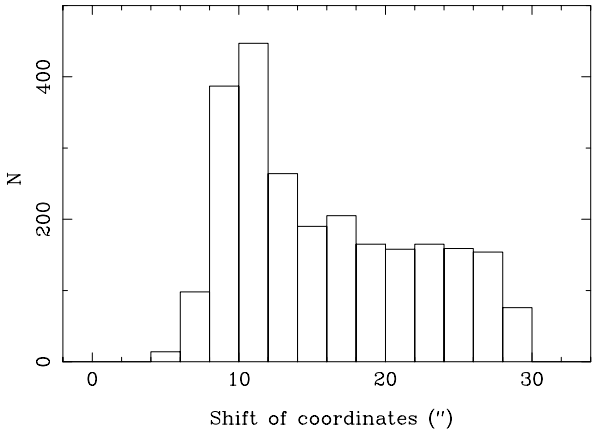

Fig. 4. Histogram of the differences between the two astrometric solutions (GSC- and direct-solution)

Class	Number of objects	percentage
Stars	500	43.6%
Galaxies	523	45.6%
Unknown	123	10.7%
Total	1146	100%

This sample will be used as a test sample (or training sample) in a discriminant analysis method (DA) for galaxy recognition.

5.2. Discriminant analysis

The DA is a common method for automatic recognition. The test sample being shared in $n_{\rm c}$ classes $\{I_{\rm k}\}$ ($k = 1$, $n_{\rm c}$), the purpose of DA is to find the principal factorial axis on which each class is as concentrated as possible and as distinct as possible from the others. This is achieved by maximizing the inertia between classes and by minimizing the inertia within each class. Inertia is calculated from the set of parameters attached to each object. We will note p_{ij} the j-th parameter of object i.

The mathematical result (see Diday et al. 1982) is that the factorial axes are the eigenvectors of the matrix $\mathcal{T}^{-1}.\mathcal{B}$, where $\mathcal{T}$ is the total covariance matrix and $\mathcal{B}$ is the inter-class covariance matrix.

Note that the matrix $\mathcal{T}^{-1}.\mathcal{B}$ is not symmetrical and that the total covariance matrix is the sum of the intra-class covariance matrix $\mathcal{W}$ (covariance Within class) and of inter-class covariance matrix $\mathcal{B}$ (covariance Between class). This is called the Huyghens decomposition.

$$\mathcal{T} = \mathcal{W} + \mathcal{B}. \tag{1}$$

The elements of $\mathcal{B}$ are:

$$b_{jj'} = \sum_{k=1}^{n_c} \frac{N_k}{N} (\overline{p_j^k} - \bar{p_j})(\overline{p_{j'}^k} - \bar{p_{j'}}) \tag{2}$$

where N_k is the number of objects in the class I_k ($k = 1$ to n_c), where the mean parameter j for the whole sample is:

$$\bar{p_j} = \frac{1}{N} \sum_i p_{ij} \tag{3}$$

(N is the number of objects of the whole sample), and where the mean parameter j within the class $\{I_k\}$ is:

$$\overline{p_j^k} = \frac{1}{N_k} \sum_{i \in I_k} p_{ij}. \tag{4}$$

The elements of the total covariance matrix $\mathcal{T}$ are:

$$t_{jj'} = \sum_k \frac{1}{N} \sum_{i \in I_k} (p_{ij} - \bar{p_j})(p_{ij'} - \bar{p_{j'}}). \tag{5}$$

Now, we have to choose the set of parameters attached to each object.

5.3. Choice of discriminant parameters

Any discriminant method requires a good choice of discriminant parameters which are used for the definition of the metric. These parameters are not necessarily independent but they must cover all features which seem relevant for a reliable discrimination of astronomical objects. For galaxy recognition we tested 7 parameters.

1. Peak intensity per area unit, this is Peak intensity divided by the surface of the considered object.
2. Mean surface brightness, total flux divided by area.
3. Peak intensity.
4. Axis ratio, ratio of the major to the minor axis.
5. Relative area, ratio of number of pixels of the object and of the matrix.
6. Elongation of the matrix.
7. Presence of diffraction cross.

The DA method is applied on half the sample (i.e. 573 objects) and tested on the other half using only one parameter at a time (in this case the factorial axis is defined by the parameter itself). The percentage of good results is given below for each one, individually.

Parameter	stars	galaxies	mean
Peak over area	100.0%	98.9%	99.4%
Mean SB	98.7%	99.6%	99.2%
Peak intensity	96.2%	98.5%	97.4%
Axis ratio	83.7%	54.8%	69.2%
Relative surface	77.0%	58.5%	67.7%
Elongation of matrix	88.3%	40.8%	64.5%
Diffraction Cross	68.2%	57.0%	62.6%

The conclusion of this test is that the most relevant information about the nature of an object is contained in the pixel intensity, not in the shape of the object. Stars have a very high central intensity, galaxies do not. Moreover, stars are concentrated, galaxies are not. This explains why "Mean SB" and "Peak over area" give such an impressive recognition rate. Finally, only the first four parameters have been used. The axis ratio is kept because it becomes relevant for faint objects despite that its rate is relatively low.

5.4. Result

The DA method is applied with the four parameters described above and three classes "Galaxies", "Stars" and "unknown objects". Using the test sample, each object is projected onto the first factorial axis. Figure 5 shows the projection onto the first factorial axis of "Galaxies" and "Stars" classes. Similar plots exists for "Stars" and "unknown objects" classes and for "Galaxies" and "unknown objects" classes. All "unknown objects" have been eliminated in the next part of this study.

One can see that there is an overlapping region where "Galaxies" and "Stars" are mixed. The limits of this zone can be tuned in such a way that one can accept a given percentage of misclassification. We choose 0% chance of classifying a star as a galaxy and 5% chance of classifying a galaxy as a star. Indeed, it is important to avoid the contamination of the catalog by stars while it is not as important to miss a galaxy (which is uncertain anyway). These limits are drawn in Fig. 5 where it is visible that no star enter the galaxy-domain, while 5% of galaxies enter the star-domain. Objects between these two limits will be classified as undefined.

5.5. Visual control

The final step of this treatment consists in checking visually all frames recognized as galaxies. This tedious part allows us to reject artefacts (1148 rejections after the inspection of 54073 images) like those produced by star halos truncated by the edge of the frame. Such truncated halos look like elongated, low-surface brightness object, easily accepted as galaxies.

As a result, a code is given to describe three features:

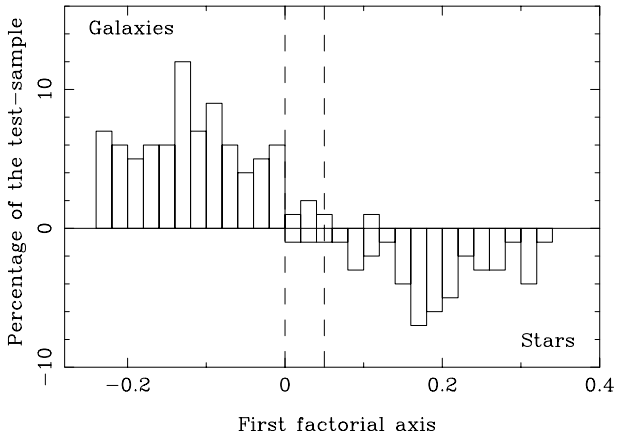

Fig. 5. Definition of acceptation zones along the first factorial axis. The left-hand zone defines "Galaxies", the righthand one defines "Stars", and the intermediate one defines "undefined objects"

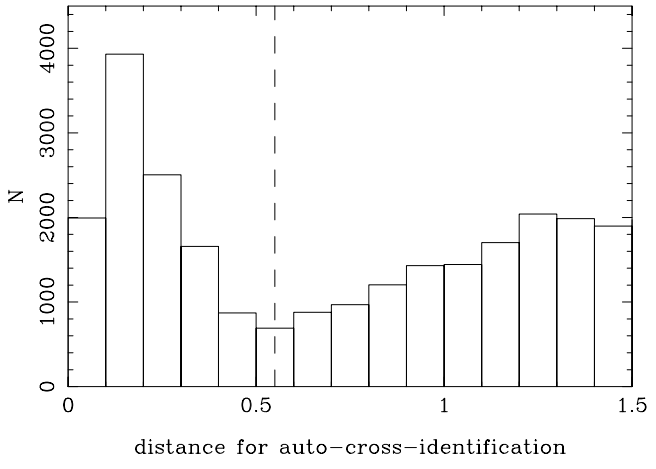

Fig. 6. Distribution of "distances" d_{ij} between two DENIS objects (i and j). This graph is used to chose $d_{\rm limit}$ in the auto-cross-identification phase (see text)

– "multiple", if several objects are present in the matrix
– "truncated", if the galaxy is truncated by the edge of the array.
– "peculiar", if the galaxy looks strange for any reason.

So, each galaxy of the catalog has been inspected visually. This will prevent us from gross misidentification. Now, the galaxies have to be cross-identified with known galaxies.

6. Cross-identification

To make a correct cross-identification we need coordinates, calibrated magnitudes and diameters, axis ratios and position angles. We will use the first calibration obtained from the preliminary cross-identification made for astrometric purposes (Sect. 4). This calibration will be refined in next section.

Because of frame overlap along the strip, many objects are measured twice (or even three or four times with adjacent strips). A first cross-identification is done for these galaxies measured several times. This will be called the "auto-cross-identification". Then, the cross-identification with LEDA galaxies may start.

6.1. Auto-cross-identification

The "auto-cross-identification" is performed using a hierarchical method in which we merge step by step the closest objects. The definition of the distance of two objects i and j is the following:

$$d_{ij} = \frac{1}{n_{\rm p}} \sum_{k=1}^{n_{\rm p}} \frac{|p_{ik} - p_{jk}|}{2\sigma_k} \qquad (6)$$

where, $n_{\rm p}$ is the number of parameters (coordinates, diameters magnitudes...) for a given object, p_{ik} is the k-th parameter of object i, σ_k is the standard error of the k-th parameter. When two objects are merged they are replaced by a single one, whose parameters are the means of both. The final result does not depend on the order the original file is read. Note that, special care must be taken for periodic parameters, Right ascension and position angle (e.g., PA = 0 deg is identical to PA = 180 deg; thus, the mean of PA = 3 deg and PA = 177 deg is PA = 0 deg, not PA = 90 deg).

The adopted σ_k are given in the following table:

Parameter	σ_k
α_{2000}	$30''$
δ_{2000}	$30''$
$\log D$	0.08
$\log R$	0.08
$I_{\rm T}$	0.3 magnitude
β	$5/\log R$ degree

The standard error of the position angle is taken as a function of $\log R$ because its meaning vanishes for face-on galaxies.

Objects are merged for $d_{ij} < d_{\rm limit}$, $d_{\rm limit}$ beeing chosen from the distribution of all distances (Fig. 6). By its definition, d_{ij} has the meaning of a Student's t-test devided by 2 (it is thus dimensionless). A 1σ criterion corresponds roughly to $d_{\rm limit} = 0.5$. However, the value of σ attached to each parameter is somewhat arbitrary, so is the definition of $d_{\rm limit}$. We adopted $d_{\rm limit} = 0.55$. This choice is guided by the minimum observed in the histogram of d_{ij} (Fig. 6).

During "auto-cross-identification" a provisional DENIS number (called RED) is given to each entry of the catalog. When a galaxy appears several times in the catalog, each original set of measurements is identified with the same RED number. Each entry will be cross-identified independently with LEDA galaxies,

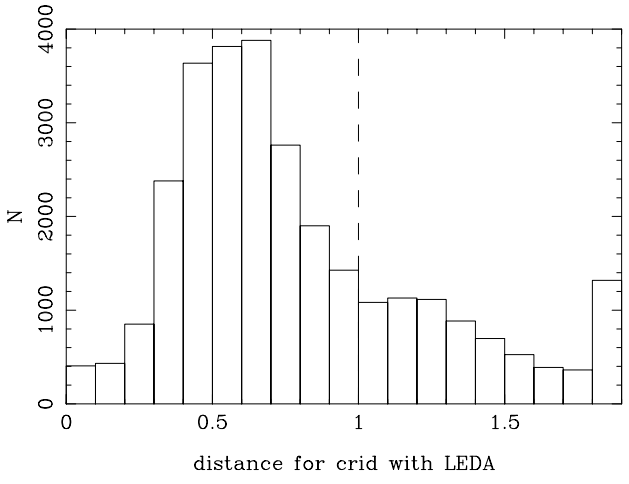

Fig. 7. Distribution of "distances" d_{ij} between DENIS and LEDA galaxies (i and j). This graph is used to chose $d_{\rm limit}$ in the cross-identification phase (see text)

this will allow us to check the reliability of the cross-identification.

6.2. Cross-identification with LEDA galaxies

From the previous step we get an intermediate catalog in which each galaxy has a provisional number and all its astrophysical parameters (α_{2000}, δ_{2000}, $\log D_{\rm I}$, $\log R_{\rm I}$, $I_{\rm T}$ and β). Each entry of this catalog must now be cross-identified with LEDA galaxies in order to identify those already known.

LEDA galaxies have similar parameters α_{2000}, δ_{2000}, $\log D_{25}$, $\log R_{25}$, $B_{\rm T}$ and β, but diameters and magnitudes are defined in the photometric B-band. The cross-identification is done by calculating the distance (in the mathematical sense, as defined by Eq. (6)) between a DENIS and a LEDA galaxy. The coincidence is accepted if the distance is smaller than $d_{\rm limit}$. From a histogram of all distances between LEDA and DENIS measurements (Fig. 7), we adopted $d_{\rm limit} = 1.0$ which corresponds to the first minimum of d_{ij}-histogram (a pure Student's t-test would have given $d_{\rm limit} = 1.29$ at a 0.01 probability level). This limit is voluntarily conservative (i.e., small) because we prefer to miss a cross-identification than to merge two distinct galaxies.

Because a given galaxy is cross-identified each time it appears in the catalog, 15945 were cross-identified several times with their original parameters. We reject 1881 galaxies identified with more than one LEDA galaxy. The final catalog contains now 36247 galaxies.

6.3. Last cleaning

Many objects were kept in the catalog despite the fact that they were labelled "undefined objects" by the DA. They were kept because a known galaxy was very close. In the present release we removed these objects which nature may be questionable without further inspection. Indeed, some very faint galaxies in LEDA have only a few parameters, so that the cross-identification is based mainly on coordinates. In some crowded field (clusters of galaxies or low galactic latitude) the accuracy of coordinates does not allow an identification secure enough. 10696 such objects were then rejected, leaving 25551 galaxies.

Finally, we rejected galaxies with uncertain coordinates so that only coordinates based on the GSC reference are used. So, 5291 galaxies are rejected in the present version, leading to the final catalog of 20260 galaxies. These drastic rejections aim at maintaining a high quality level for this first catalog. In order to judge the quality more quantitatively we will now compare with other sources of data.

7. Comparison with Mathewson et al. samples

7.1. Magnitudes

Magnitudes are calibrated by comparison with the measurements in I-band photometry made by Mathewson et al. (1992, 1996) which gives access to 2441 galaxies. This comparison allows us to correct for a possible variation of the zero-point. This variation has been explained by seasonal variation of the mean temperature of the camera[1]. Figure 8 shows such a variation described by the parameter C:

Night number	C
1850 − 2150	+0.05
2151 − 2350	−0.08
2351 − 2600	+0.03
2600 − 2800	−0.05

Note that the "night number" is a logical number, not a real night number. Each time the system is initialized the night number is incremented. This explains that after one year of running survey there are 2500 logical nights.

An airmass correction is adopted using a typical value $\Delta I/\Delta \sec\zeta = 0.04 \pm 0.02$. A check is made to control that there is no airmass residual. The residual is smaller than 0.01 magnitude. The DENIS I-magnitude is then:

$$I(\text{DENIS}) = -2.5 \log\left(\sum_{i=1}^{n} f_{ij} - f_{\rm bg}\right) + 24.01 - 0.04\ \sec\zeta + C. \quad (7)$$

[1] The camera is now equiped with a regulated cooling system.

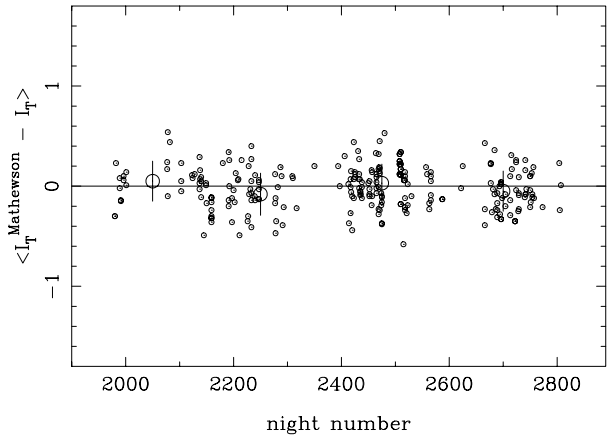

Fig. 8. Zero-point variation obtained by comparison with Mathewson's I-band photometry

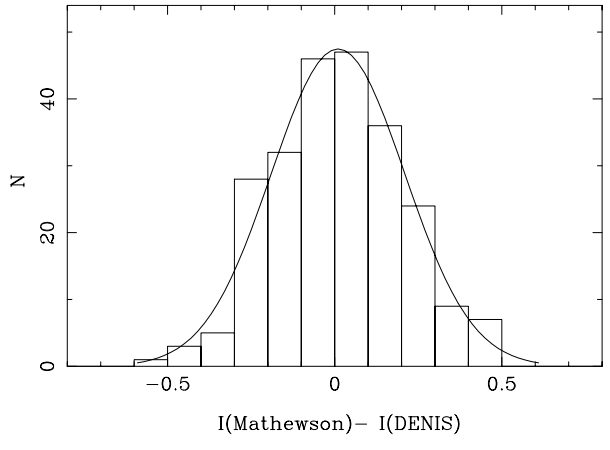

Fig. 9. Zero-point distribution after a tiny seasonal correction

The zero-point distribution of I(Mathewson) $-I$(DENIS) is Gaussian (Fig. 9) with a standard deviation of 0.2 magnitude. If we assume that the error is identical for both systems the mean error on DENIS extragalactic I-band magnitudes would be about 0.14 magnitude. Because the uncertainty on Mathewson et al. data is probably smaller, the uncertainty on our I-band magnitudes is about $\sim$0.18 magnitude.

In Fig. 10, the comparison between I(Mathewson) and I(DENIS) is shown for galaxies with secure identification and being neither "multiple" nor "truncated". The direct regression is:

$$I(\text{Math.}) = 1.05 \pm 0.02 I(\text{DENIS}) - 0.54 \pm 0.24 \quad (8)$$

with the following standard deviation, correlation coefficient and number of objects: $\sigma = 0.21$, $\rho = 0.977 \pm 0.004$, $n = 163$ after 11 rejections at 3σ.

Stricto sensu, the slope is not significantly different from 1, and the zero-point is not significantly different from 0. So, we are keeping the conservative solution: I(Math.) $\equiv I$(DENIS). Among the 10 rejected galaxies, 8 can be explained by localized poor photometric conditions (because they correspond to a loss of flux). The measurements of corresponding nights will be counted with half

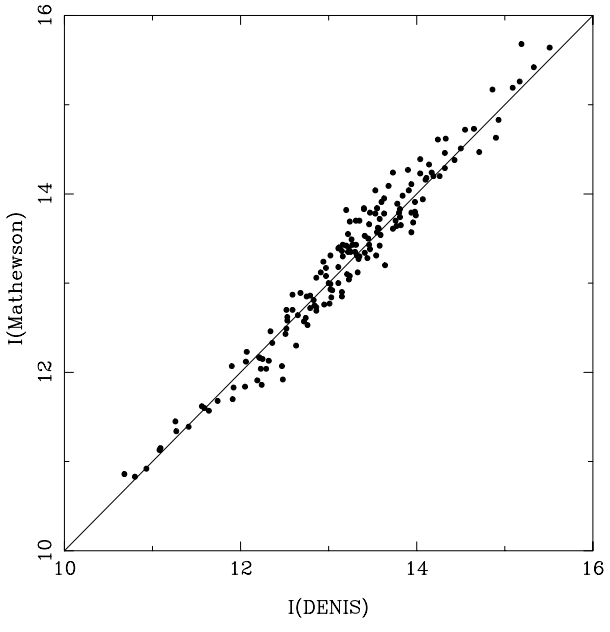

Fig. 10. Comparison of extragalactic I-band magnitudes from Mathewson et al. and from DENIS

weight. Two nights were rejected (night 2475 and 2159) because they give rejections in the comparison of different photometric parameters.

7.2. Diameters and axis ratios

Diameters and axis ratios are also compared with those of Mathewson et al. samples. These comparisons are given in Fig. 11 and Fig. 12, respectively. The direct regression are:

$$\log D(\text{Math.}) = 0.96 \pm 0.04 \log D(\text{DENIS}) + 0.04 \pm 0.04 \quad (9)$$

with $\sigma = 0.10$, $\rho = 0.88 \pm 0.02$, $n = 170$ after 4 rejections at 3σ.

For the axis ratio, it is better to force the intercept to be zero as generally admitted (see de Vaucouleurs et al. 1976). This avoids to have negative axis ratio after the application of the regression. The result is thus:

$$\log R(\text{Math.}) = 0.94 \pm 0.04 \log R(\text{DENIS}) \quad (10)$$

with $\sigma = 0.10$, $\rho = 0.85 \pm 0.02$, $n = 172$ after 2 rejections at 3σ. None of these regressions is significantly different from the absolute identity. So, we will keep: $\log D$(Math.) $\equiv \log D$(DENIS) and $\log R$(Math.) $\equiv \log R$(DENIS). The standard deviations are 0.10 for both $\log D$ and $\log R$. Again, if we assume the same error on both systems the error on $\log D$ and $\log R$ is about 0.07.

8. Comparison with LEDA galaxies

8.1. Equatorial coordinates

The coordinates are compared with coordinates given in LEDA. Only coordinates known as "accurate"

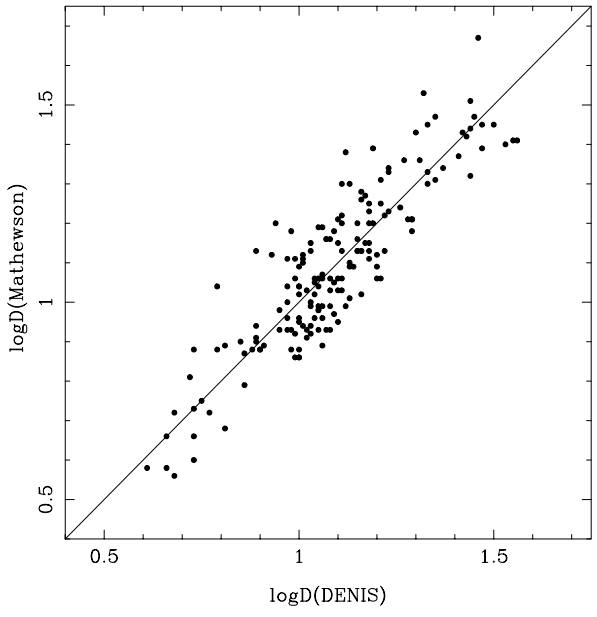

Fig. 11. Comparison of I-band isophotal diameters from Mathewson et al. and from DENIS

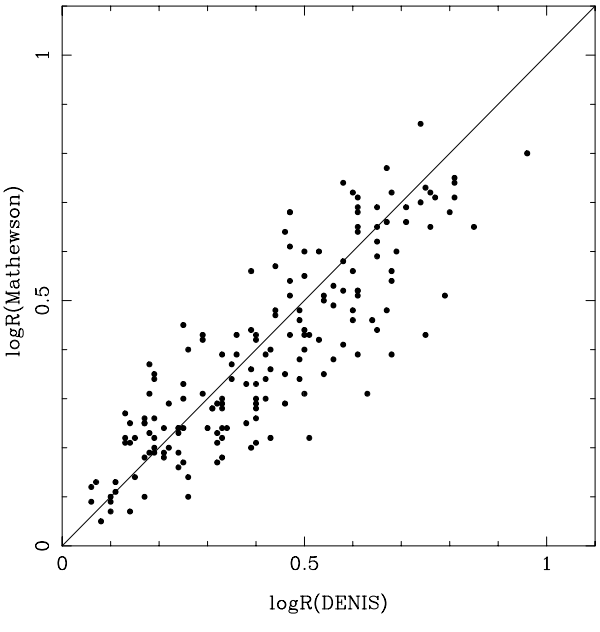

Fig. 12. Comparison of I-band axis ratios from Mathewson et al. and from DENIS

in LEDA (i.e. with a standard deviation less than 10 arcsec) are used. The plot of $\Delta\delta$ and $\Delta\alpha.\cos\delta$ in Fig. 13 shows that there is no systematic distorsion (Δ means (DENIS)−(LEDA)). The standard deviation is 6.5 arcsec and 6.7 arcsec for $\alpha.\cos\delta$ and δ, respectively. Assuming an error of the same amplitude in LEDA and DENIS coordinates gives an uncertainty of $6.6/\sqrt{2}$ arcsec for DENIS right ascension and declination, i.e. an uncertainty of 6.6 arcsec for the position of a galaxy.

In fact, the plot of $\Delta\alpha\cos\delta$ vs. $\Delta\delta$ exhibited two abnormal zones with a systematic shift of about 30 or

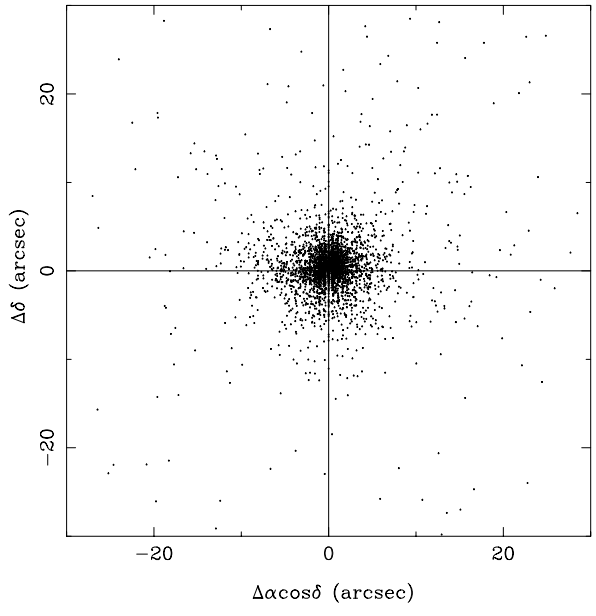

Fig. 13. Comparison of coordinates from LEDA and DENIS.

40 arcsec. This problem appeared near the zenith. Thus, only objects with coordinates based on the GSC stars are kept in the present version. In the final catalog, the coordinates will be obtained through a full astrometric solution (mosaicing frames along each strip and with adjacent ones) and this problem will be solved without rejecting galaxies.

8.2. Position angle

Position angle is important for studies on the orientation of galaxies, but also for identification. However, for nearly face on galaxies, it becomes very uncertain. The comparison is made only for galaxies with $\log R(\mathrm{DENIS}) > 0.5$. The result is given in (Fig. 14). The direct regression gives:

$$\beta(\mathrm{LEDA}) = 1.009 \pm 0.003\beta(\mathrm{DENIS}) + 0.07 \pm 0.26 \quad (11)$$

with $\sigma = 2.65$, $\rho = 0.9987 \pm 0.0001$, $n = 408$ after 21 rejections at 3σ. Among the 21 rejections, only 2 correspond to real discrepancies.

The uncertainty on the measurement of β is 2.7 deg. This excellent agreement of position angles validates the reliability of our cross-identification.

8.3. Photometric morphological type code

It is interesting to obtain at least a very crude estimate of the morphological type code. This is particularly important when we plan to start a HI follow-up for which it is compulsory to avoid elliptical galaxies. The log of the standard deviation of pixel intensities is significantly correlated with the morphological type code extracted from LEDA. The relation is almost linear. However, it appears

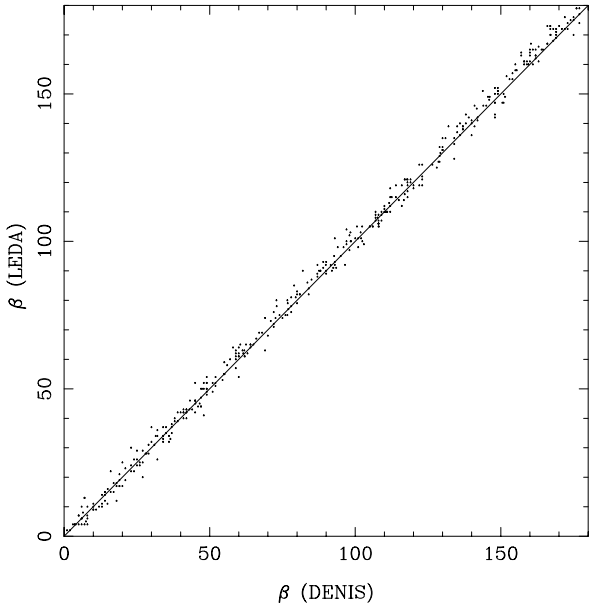

Fig. 14. Comparison of position angles from LEDA and DENIS

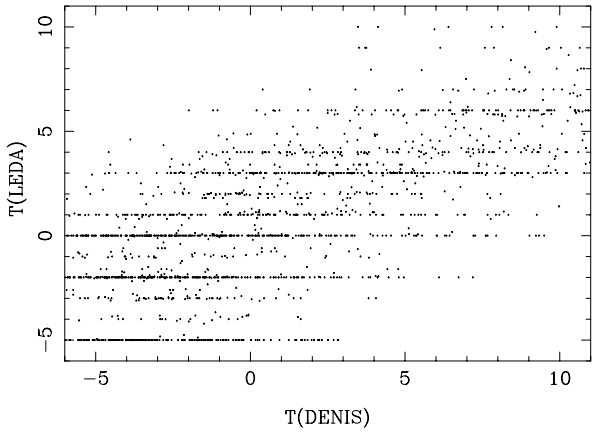

Fig. 15. Comparison of morphological type codes from LEDA and from the I-band photometry

that the solution depends on the size of the galaxy (all very small objects appear identical). The slope and the intercept are found linearly correlated with the log of the number of pixels. In the scale between −5 and 10 defined in the Second Reference Catalog of Bright Galaxies, the photometric morphological type code is calculated as:

$$T(\mathrm{DENIS}) = A\,\log(\sigma(f_{ij})) + B. \quad (12)$$

Where $\sigma(f_{ij})$ is the standard deviation of flux of all pixels of the matrix representing the galaxy:

$$\sigma(f_{ij})) = \sqrt{\frac{\sum_{i,j}(f_{ij} - \bar{f})^2}{(n-1)}} \quad (13)$$

with

$$A = \frac{1}{-0.0187\,\log n - 0.0183} \quad (14)$$

$$B = \frac{1}{0.2774\,\log n + 1.7846} \quad (15)$$

where n is the number of pixels.

The comparison of codes T(DENIS) and T(LEDA) is given in Fig. 15. The correlation is clearly significant (the correlation coefficient is $\rho = 0.69 \pm 0.01$) but the standard deviation is large ($\sigma(T(\mathrm{DENIS})) = 2.5$). This allows us to classify galaxies into "Early", "Intermediate" and "Late" types, with no finer subdivision. In the catalog, photometric morphological type smaller than −5 or greater than 10 will be set to −5 or 10, respectively.

9. The catalog

9.1. Description of the catalog

The catalog of galaxies which is described here is the first of a series which will be released during the progression of the survey. At the end of the survey a deeper and complete catalog will be produced at PDAC. The present one, is necessarily limited to the first observations (one year).

The catalog contains 20260 galaxies. Among them 14518 are new galaxies while 5742 are galaxies already present in LEDA.

Each galaxy is numbered with a provisional internal number (RED, for Rapid Extraction from DENIS), and an identifier from the LEDA database (PGC/LEDA)[2]. Galaxies are also identified with an alternate name taken in the following catalogues: NGC, IC (Dreyer 1988), UGC (Nilson 1973), ESO (Lauberts 1982), MCG (Vorontsov-Velyaminov et al. 1962-1974), CGCG (Zwicky et al. 1961-1968), IIZW, IIIZW, VIII from the catalog of compact and eruptive galaxies (Zwicky 1971), IISZ (extension of the same list by Rodgers et al. (1978), FAIR (Fairall 1977-1988), HICK (Hickson 1989), KUG (Takase & Miyauchi-Isobe 1984-1989), IRAS (IRAS), MK (Markarian 1971-1977), UM (University of Michigan list, MacAlpine et al. 1981). The detailed references to these catalogs are given in Paturel et al. (1989). Two additional catalogs are included: Saito et al. (1990-1991) and Dressler (1980). The notations for corresponding galaxy names are SAIT (e.g. SAIT 69-1, for object 69 in list 1 of Saito et al.) and DRCG (e.g., DRCG 39-41, for galaxy 41 in cluster 39, the numbering of clusters is made according to the order in the original publication).

For each galaxy, the catalog gives the weighted mean parameters obtained as described in the previous section. Actual mean errors σ are calculated according to Paturel et al. (1996) using individual mean errors deduced in previous section. For I-band magnitudes the mean error is taken as a function of the magnitude itself. An estimate made from Fig. 10 gives: $\sigma(I) = 0.05 B_{\mathrm{T}} - 0.51$.

[2] Connection:
http://www-obs.univ-lyon1.fr/leda
or
telnet: lmc.univ-lyon1.fr **login:**leda

The weights used for calculating the weighted means are the inverse square of actual mean errors. For nights suspected to be of poor photometric quality the actual mean error is divided by 3[3]. Further, when the quality of the matrix is uncertain ("peculiar", "multiple" or "truncated"), the weight is divided by 2. This correcting coefficient is deduced from the comparison of I magnitudes with poor quality objects.

The quality of each individual matrix is coded as follows: "Normal" galaxies are coded as 1, "Peculiar" galaxies as 10, "Multiple" as 100 and 'Truncated' as 1000. This code is added for each measurement. So, the resulting code gives immediately the number of independent measurements (sum of digits) and the quality of each of them. For instance, the code 1002 means that there are one truncated matrix and two normal ones (i.e., 3 independent measurements). "Truncated" means an overestimated magnitude, on the contrary, "Multiple" means that the magnitude of the considered galaxy is underestimated.

The different columns are the following:

- **Column 1:** Provisional DENIS identifier. This identifier is just an internal number given for easy identification. This number will be replaced by an appropriate final DENIS number.
- **Column 2:** LEDA identifier. This number allows rapid retrieval in the LEDA database. This number is identical to the PGC number for LEDA number less than 73197.
- **Column 3:** Alternate name according to a hierarchy: NGC, IC, ESO, UGC, MCG (see text above).
- **Column 4:** Equatorial coordinates for epoch 2000, in hours, minutes, seconds and tenths for the Right Ascension and in degrees, arcminutes and arcseconds for the declination. The actual mean error on the position of the galaxy is given in the same column, next line in arcseconds.
- **Column 5:** Total I-band magnitude $I(DENIS)$ with its mean error on the second line.
- **Column 6:** Isophotal diameter in log scale $\log D$(DENIS), where D is in 0.1 arcmin following the notation of de Vaucouleurs et al. (RC1, RC2). The actual mean error is given on the second line.
- **Column 7:** Isophotal axis ratio in log scale $\log R$(DENIS), where R is the ratio of the major to the minor axis. The actual mean error is given on the second line.
- **Column 8:** Position angle β(DENIS) in degrees, measured from North Eastwards. Its value lays between 0 and 180 degrees (excluding 180). For $\log R$(DENIS) < 0.5 the meaning is poor. This is reflected by the actual mean error given on the second line.
- **Column 9:** Photometric morphological type code T(DENIS). The coding is given according to RC2 (i.e. T from -5 to 10 for Elliptical to Irregular galaxies). The mean error is given on the second line.
- **Column 10:** Quality code of the object (1000 = truncated object, 100 = multiple object, 10 = peculiar object, 1 = normal galaxy). The sum of digits gives the number of independent measurements.

A sample page is given at the end of the paper. The catalog is available in electronic form at PDAC and Lyons Observatory.

9.2. Distribution on the sky

The distribution on the sky is given in equatorial coordinates for the epoch 2000 (Fig. 16). The strips are clearly visible. The zone called "Equatorial" (δ between $+2$ deg and -28 deg) is not so well covered because observations are avoided in this zone when Moon is bright or when the wind is strong. Further, many frames are rejected in this zone at the end of the strip (near -28 deg) because of the shift in header-coordinates. No attempt is made to reach low galactic latitudes. This is done independently in J and K bands.

9.3. Completeness limit

If we assume a homogeneous distribution of galaxies ($N \propto r^3$), the plot of the number of galaxies (in log scale, i.e. $\log N$) brighter than a given magnitude limit $I_{\rm limit}$ versus this magnitude limit should be linear with a slope of 0.6. This plot (Fig. 17) is quite linear up to $I_{\rm limit} = 14.5$ with a slope of 0.62 ± 0.02. The sense of this completeness limit must be explained. It means that in surveyed directions all galaxies brighter than 14.5 are detected. Because the sampling is made randomly and 1/4 of the survey is presented here, the completeness limit in apparent magnitude of this first DENIS catalog is $I_{\rm limit} = 14.5$.

Acknowledgements. This work would have been impossible without the collaboration of M.C. Marthinet, C. Petit, L. Provost, F. Gallet, R. Garnier, J. Rousseau. They are fully associated with this work. The DENIS team is warmly thanked for making this work possible and in particular the Operations team at la Silla. We thank also G. Mamon for careful reading of the article. The DENIS program is partly funded by the European Commission through *SCIENCE* and *Human Capital and Mobility* grants. It is also supported in France by INSU, the Education Ministry and CNRS, in Germany by the Land of Baden-Würtenberg, in Spain by DGICYT, in Italy by CNR, in Austria by the Fonds zur Förderung der Wissenschaft und Forschung, in Brazil by FAPESP.

[3] These nights were detected by a 3σ rejection rule, so one can admit that their mean error is three times the typical mean error.

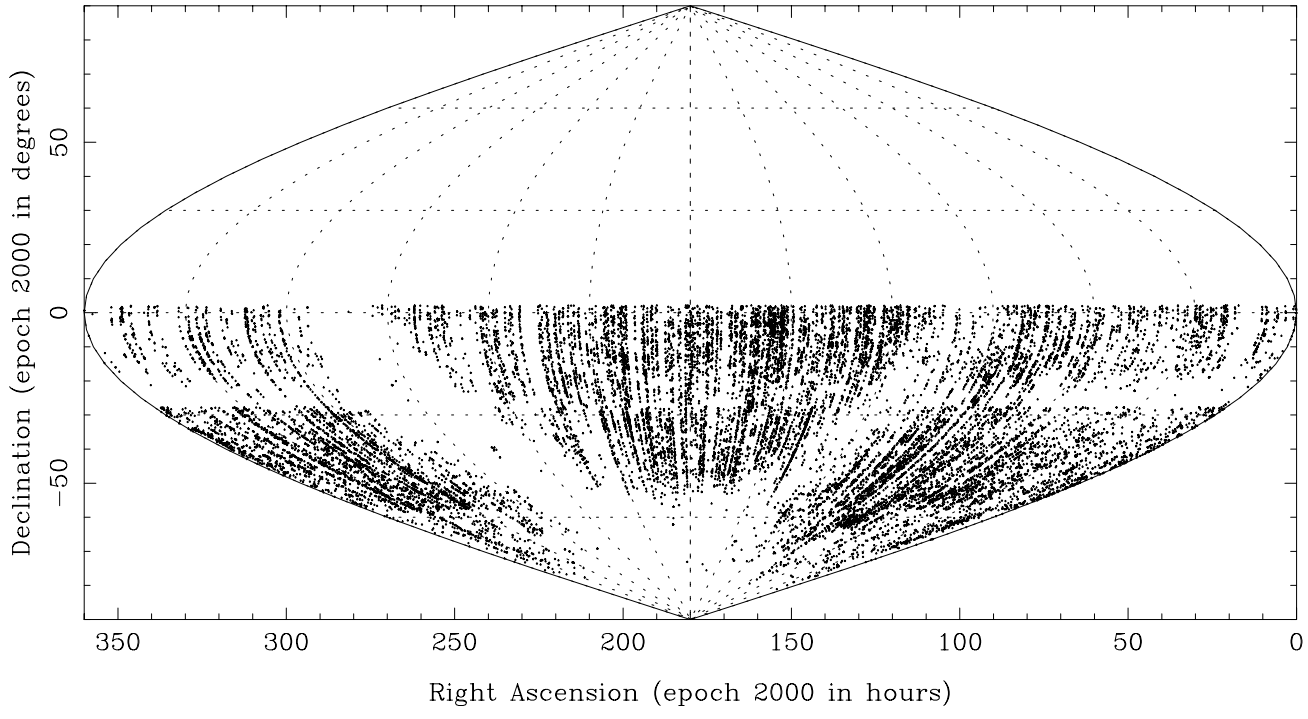

Fig. 16. Distribution of the 20260 galaxies of the present DENIS catalog presented with a Flamsteed's equal area projection in equatorial (2000) coordinates

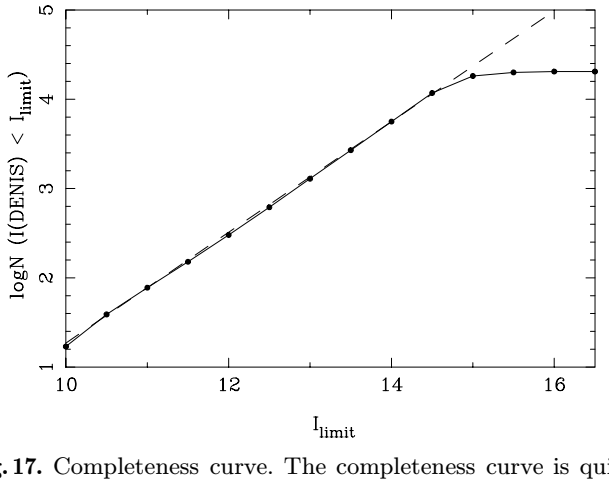

Fig. 17. Completeness curve. The completeness curve is quite linear up to the completeness limit $I_{\rm limit} = 14.5$. The slope (0.62 ± 0.02, dashed line) is very nearly the one expected for a homogeneous distribution of galaxies (0.6)

References

Diday E., Lemaire J., Pouget J., Testu F., 1982, "Éléments d'analyse de données". Dunod, Paris, ISBN 2-04-015430-2

Dressler A., 1980, ApJS 42, 565

Epchtein N., 1998, "The impact of near infrared surveys on galactic and extragalactic astronomy", Proc. 3rd. Euroconf. Kluwer ASSL Series 230

Epchtein N. + 47 authors, 1997, The Messenger No. 87, p. 27

Garzón F., Epchtein N., Omont A., Burton W.B., Persi P., 1997, "The impact of large-scale near-infrared sky surveys", ASSL Series, Vol. 210. Kluwer Acad. Pub., Dordrecht

Guide Star Catalog, 1989-1992, Space Telescope Science Institute (GSC)

Lebart L., Fénelon J.P., 1975, "Statistique et Informatique Appliquées". Eds. Bordas, Paris

Mathewson D.S., Ford V.L., Buchhorn M., 1992, ApJS 81, 413

Mathewson D.S., Ford V.L., 1996, ApJS 107, 97

Paturel G., Fouqué P., Bottinelli L., Gouguenheim L., 1989, A&AS 80, 299

Paturel G., Garnier R., Petit C., Martinet M.C., 1996, A&A 311, 12

Paturel G., Andernach H., Bottinelli L., et al., 1997, A&AS 124, 109

Saito M., et al., 1990, PASJ 42, 565

Saito M., et al., 1991, PASJ 43, 449

de Vaucouleurs G., de Vaucouleurs A., Corwin H.G. Jr., 1976, Second Reference Catalog of Bright Galaxies. University of Texas Press, Austin (RC2)

de Vaucouleurs G., de Vaucouleurs A., Corwin H.G. Jr., Buta R.J., Paturel G., Fouqué P., 1991, Third Reference Catalog of Bright Galaxies. Springer-Verlag (RC3)

Table 1. Sample page of the present catalog

DENIS-RED (1)	LEDA/PGC (2)	Alternate Name (3)	R.A. DEC.(2000) (4)	I (5)	logD (6)	logR (7)	p.a. (8)	T (9)	code (10)
000142	000087	DRCG 39- 41	J000109.8-503505	14.82	.718	.306	42.9	0.	2
			5	.17	.061	.057	5.5	2.	
000149	143168		J000110.8-404542	12.97	.873	.083	17.0	-4.	1
			6	.14	.070	.070	19.0	3.	
000150	143169		J000111.7-384507	15.45	.733	.486	102.0	6.	1
			6	.26	.070	.070	3.9	3.	
000153	124807		J000112.3-391354	14.99	.648	.188	95.9	-1.	2
			4	.21	.052	.080	21.5	3.	
000159	143172		J000115.9-730851	15.28	.683	.417	120.0	-2.	1
			6	.36	.099	.099	6.4	4.	
000160	000099	ESO 149- 12	J000117.5-530033	13.54	1.138	.701	36.9	4.	2
			5	.12	.050	.054	2.2	2.	
000165	143175		J000119.7-523551	14.29	.828	.389	14.1	10.	2
			5	.15	.067	.051	4.0	2.	
000168	143177		J000120.4-404721	14.70	.713	.236	44.0	1.	1
			6	.23	.070	.070	7.7	3.	
000170	143179		J000121.0-723533	14.97	.683	.181	134.0	0.	1
			6	.24	.070	.070	9.9	3.	
000174	130913		J000131.1-404912	13.99	.873	.208	114.0	10.	1
			6	.19	.070	.070	8.7	3.	
000182	124990		J000138.5-435949	14.51	.663	.000	153.0	-2.	1
			6	.22	.070	.070	90.9	3.	
000183	124811		J000139.9-383834	15.59	.543	.264	46.0	2.	1
			6	.27	.070	.070	7.0	3.	
000226	143200		J000200.1-515740	14.64	.713	.181	39.0	0.	1
			6	.22	.070	.070	9.9	3.	
000253	143209		J000218.6+015033	14.53	.683	.181	134.0	-4.	1
			6	.22	.070	.070	9.9	3.	
000272	143215		J000233.8-111705	14.31	.903	.458	78.0	3.	1
			6	.21	.070	.070	4.2	3.	
000289	000205	UGC 5	J000305.7-015449	12.18	1.248	.354	51.5	5.	2
			5	.07	.052	.069	4.2	2.	
000292	143223		J000307.6-160643	14.64	.723	.153	90.0	3.	1
			6	.22	.070	.070	11.4	3.	
000293	143224		J000308.6-170300	14.55	.683	.125	83.0	-2.	1
			6	.22	.070	.070	13.6	3.	
000294	143225		J000309.0-195221	15.00	.703	.431	19.0	-5.	1
			6	.24	.070	.070	4.4	3.	
000296	000211		J000310.5-544457	12.23	1.135	.167	58.1	-4.	1001
			6	.10	.071	.078	9.9	3.	
000299	143226		J000313.5-512806	14.78	.743	.417	142.0	0.	1
			6	.23	.070	.070	4.6	3.	
000303	143228		J000318.3-131618	14.16	.923	.417	83.0	10.	1
			6	.20	.070	.070	4.6	3.	
000307	143229		J000320.4-394823	14.96	.783	.486	131.0	3.	1
			6	.24	.070	.070	3.9	3.	
000309	000224	FAIR 627	J000321.3-500448	13.47	.933	.347	110.2	-4.	2
			5	.12	.053	.109	3.9	2.	
000310	073217		J000321.4-543338	12.81	1.023	.125	145.0	-2.	100
			20	.39	.210	.210	40.8	9.	
000311	143230		J000321.6-190604	14.74	.733	.306	146.0	-2.	1
			6	.23	.070	.070	6.1	3.	
000313	143232		J000322.4-434615	14.73	.693	.208	165.0	-2.	1
			6	.23	.070	.070	8.7	3.	